
Selectivity in Multiple-Quantum Spectroscopy

G. Drobny, A. Pines, S. Sinton, W. S. Warren and D. P. Weitekamp

Phil. Trans. R. Soc. Lond. A 1981 **299**, 585-592

doi: 10.1098/rsta.1981.0036

Email alerting service

Receive free email alerts when new articles cite this article - sign up in the box at the top right-hand corner of the article or click [here](#)

To subscribe to *Phil. Trans. R. Soc. Lond. A* go to: <http://rsta.royalsocietypublishing.org/subscriptions>

Selectivity in multiple-quantum spectroscopy

BY G. DROBNY, A. PINES, S. SINTON, W. S. WARREN AND D. P. WEITEKAMP

*Department of Chemistry and Materials and Molecular Research Division,
Lawrence Berkeley Laboratory, University of California, Berkeley, California 94720, U.S.A.*

In multiple-quantum n.m.r. spectroscopy of N coupled spins one obtains n -quantum Fourier transform spectra, where $n = 0, 1, 2, \dots, N$. The spectra of particular interest are often those with high n , which may be analysable for a complex molecule without the need for isotopic spin labelling. For example, the $n = N$ quantum spectrum is independent of dipolar couplings and gives the total chemical shift. For $n = N - 1$, one obtains a spectrum analogous to those from all possible singly isotopically labelled molecules (e.g. one doublet corresponding to one singly labelled species for $n = 5$ in orientated benzene) and for $n = N - 2$ all possible doubly isotopically labelled species (e.g. three triplets corresponding to three doubly labelled species for $n = 4$ in orientated benzene). For large n the intensity decreases, so an important question is whether selective excitation of n -quantum transitions is possible, namely, can one design pulse sequences such that only a particular n or set of n 's is excited? This corresponds to the absorption of only groups of n quanta. It is shown that this can indeed be achieved by employing a combination of time-reversal sequences and phase shifts. The principles of the theory are outlined and examples of experimental results for large n in solids and liquid crystals are presented. The discussion includes spectra, statistical treatment of intensities, degree of selectivity and n -quantum relaxation. Selectivity is also possible in detection and examples of the sensitivity enhancement this provides are shown.

1. INTRODUCTION

The central phenomenon described here is the selective excitation of a spectroscopic system by groups of n quanta from a coherent radiation field and the use of such excitation in multiple-quantum Fourier transform nuclear magnetic resonance. A general method for such excitation is described that requires only an intense single-frequency radiation source and assumes no prior detailed knowledge of the energy-level scheme (Warren *et al.* 1979, 1980*a, b*). The effect of this excitation sequence on a spin system initially at equilibrium is to prepare only those coherent superpositions of states for which the difference in Zeeman quantum numbers, $\Delta m = nk$, is an integral multiple of the chosen value of n . These features distinguish this means of excitation from the excitation methods used in previous time-domain multiple-quantum n.m.r. experiments (Hatanaka *et al.* 1975*a, b*; Aue *et al.* 1976; Vega *et al.* 1976; Pines *et al.* 1978) and selective sequences peculiar to systems of few spins with known couplings (Wokaun *et al.* 1977*a*; Vega 1978) or which only discriminate between even quantum processes and odd quantum processes (Wemmer 1979).

The excitation phenomenon in question depends on the systematic cycling of the phase of the radiation within the excitation period to place the system in a restricted state of coherent superposition. This is in contrast to the use of phase incrementation between successive shots, which has been used to separate the signal from different orders Δm of coherence which are simultaneously excited. Separation of simultaneously excited orders may be achieved by the methods of phase Fourier transformation (Wokaun *et al.* 1977*b*; Wemmer 1979) or time proportional phase incrementation (Drobny *et al.* 1979; Bodenhausen *et al.* 1980).

[109]

In §2 the lowest-order theory of selective excitation is described. The rationale for the phase cycling is developed in the time domain and then considered in the frequency domain. In §3 the multiple quantum Fourier-transform n.m.r. experiment is reviewed and it is demonstrated how incorporation of selective excitation leads to increased signal intensities. Experimental verification of this enhancement for proton n.m.r. of molecules orientated in liquid crystals is presented. The information content of multiple-quantum n.m.r. spectra of dipolar coupled spins is discussed in §4 and compared with the possible alternative of isotopic labelling experiments that might otherwise be necessary to simplify the single-quantum spectrum of a complex molecule.

2. SELECTIVE EXCITATION BY PHASE-CYCLED IRRADIATION

(a) Average Hamiltonian for phase cycling

Suppose that a system of coupled spins is subjected to a sequence of irradiation of length $\Delta\tau_p$, which may comprise a cycle in the sense of coherent averaging theory (Haeberlen 1976). The density operator at the end of the sequence is $\rho(\Delta\tau_p) = U_\phi(\Delta\tau_p)\rho(0)U_\phi^{-1}(\Delta\tau_p)$ and for a cyclic sequence the propagator is $U_\phi(\Delta\tau_p) = \exp(-i\mathcal{H}_\phi\Delta\tau_p)$, where \mathcal{H}_ϕ is the exact effective time-independent Hamiltonian for the sequence. The subscript ϕ denotes the phase of some pulse of the sequence with respect to the spectrometer reference frequency defining the rotating frame in which ρ is expressed. Suppose that this sequence is repeated n times with the phase of all pulses incremented by $2\pi/n$ each time. The propagator is

$$U(t_c) = U(n\Delta\tau_p) = \prod_{l=0}^{n-1} \exp(-i\mathcal{H}_{\phi(l)}\Delta\tau_p), \quad (1)$$

with

$$\phi(l) = 2\pi l/n.$$

If $\|\mathcal{H}_\phi\Delta\tau_p\| \ll 1$, the approximation

$$U(t_c) \approx 1 - i\Delta\tau_p \sum_{l=0}^{n-1} \mathcal{H}_{\phi(l)} = 1 - it_c \bar{\mathcal{H}}^{(0)} \quad (2)$$

is appropriate.

The operators $\mathcal{H}_{\phi(l)}$ are related by phase shifts, i.e. $\mathcal{H}_\phi = \exp(i\phi I_z) \mathcal{H}_0 \exp(-i\phi I_z)$. Equation (2) defines the average Hamiltonian $\bar{\mathcal{H}}^{(0)}$ for the excitation sequence. To characterize it we consider the matrix elements in some eigenbasis of I_z to see if there is any selectivity.

(b) Selectivity of average Hamiltonian for phase cycling

The matrix elements for the different \mathcal{H}_ϕ are related by the expressions

$$\langle i|\mathcal{H}_\phi|j\rangle = \exp(i\Delta m_{ij}\phi) \langle i|\mathcal{H}_0|j\rangle,$$

where $\Delta m_{ij} = m_i - m_j$. Summing over n equally spaced phases gives

$$\sum_{l=0}^{n-1} \langle i|\mathcal{H}_{\phi(l)}|j\rangle = n \langle i|\mathcal{H}_0|j\rangle \delta(nk - \Delta m_{ij}). \quad (3)$$

The elements with $\Delta m = nk$ add, while all others vanish. If the initial condition $\rho(0)$ is one of no coherence, for example equilibrium, then to first order in τ the prepared density operator contains only elements of these same orders $\Delta m = nk$.

While this argument demonstrates the selectivity of such an excitation scheme, it does not guarantee that a significant fraction of the initial magnetization will develop into coherence of

the selected orders. For this to be true, the propagator $U(t_c)$ must have substantial matrix elements between states differing by $n, 2n \dots$ in their Zeeman quantum numbers. In the linear régime, for which the selectivity holds, (2) shows that this requirement must be met by the effective Hamiltonians \mathcal{H}_ϕ . Pulse sequences giving rise to such Hamiltonians are discussed in detail elsewhere (Warren *et al.* 1979, 1980*a, b*).

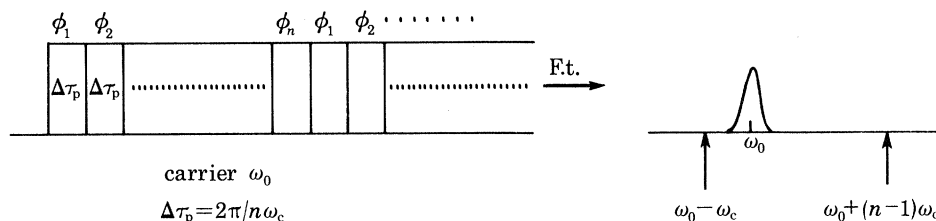


FIGURE 1. Frequency domain interpretation of selective excitation. Constant-amplitude radiation at frequency ω_0 is phase shifted by $2\pi/n$ every $2\pi/n\omega_c$ seconds. The single-quantum spectrum is centred at ω_0 . The Fourier transform of the irradiation is a comb of impulses with spacing $n\omega_c$ and an intensity maximum at $\omega_0 - \omega_c$. A resonant process at $n\omega_0$ results from a combination of n quanta, for example $(n-1)$ quanta at frequency $\omega_0 - \omega_c$ and one quantum at $\omega_0 + (n-1)\omega_c$.

(c) Frequency domain view of selective excitation

A different insight into how phase cycling leads to selective excitation can be seen in the frequency domain. If constant-amplitude irradiation at ω_0 is instantaneously phase-shifted by $2\pi/n$ every $2\pi/n\omega_c$ seconds, then its Fourier transform consists of a comb of impulses with a repeated spacing of $n\omega_c$ and intensity maximum at $(\omega_0 - \omega_c)$. This is indicated in figure 1, which shows a schematic single-quantum spectrum centred at ω_0 and the nearest frequency domain impulses. Energy conservation requires combining quanta from the frequencies above and below resonance. The resonant processes with the lowest number of quanta are those that combine n quanta with total frequency $n\omega_0$, for example the combination of $(n-1)$ quanta of frequency $(\omega_0 - \omega_c)$ with one quantum of frequency $\omega_0 + (n-1)\omega_c$. In fact the amplitude ratio for these impulses is in the same ratio of $n-1$ as the number of quanta needed from each (J. Murdoch, personal communication 1980).

3. INCORPORATION OF SELECTIVE EXCITATION INTO MULTIPLE-QUANTUM SPECTROSCOPY

(a) Multiple-quantum pulse sequence

The general form of the multiple-quantum Fourier transform experiment is indicated in figure 2. A preparation period with propagator $\hat{U}(\tau)$ acts upon the equilibrium magnetization to create some coherent superpositions of the eigenstates of \mathcal{H}_1 . These evolve for a time t_1 . After this evolution period, a mixing period with propagator $V(\tau')$ converts some of this evolved coherence back to magnetization which is observed during the detection period t_2 . Repetition of this sequence gives a signal as a function of t_1 which is a multiple-quantum free induction decay. Its Fourier transform is a multiple-quantum spectrum. This indirect method of observation is necessary because the multiple-quantum coherence does not correspond to magnetization and thus induces no voltage in the coil.

(b) *Signal intensities in the multiple-quantum experiment*

The next step is to demonstrate how selective excitation can be incorporated into this experiment to increase the signal intensity. A density operator formalism will be used to write an expression for the magnetization immediately after the mixing period. To make the calculation more symmetrical we shall write an expression for the expectation value of the longitudinal magnetization and note that the actual experiment differs from figure 2 by the addition of a $\frac{1}{2}\pi$ pulse at $t_2 = 0$ to create an oscillating transverse magnetization in t_2 .

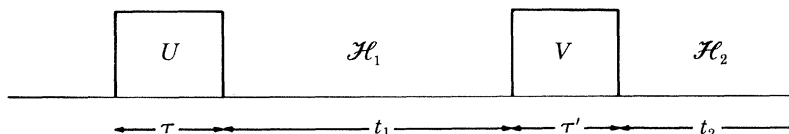


FIGURE 2. General form of a multiple-quantum Fourier transform experiment. Multiple-quantum coherent states are produced during τ , the preparation period, by the action of the propagator $U(\tau)$ upon equilibrium magnetization. These coherent states then evolve under \mathcal{H}_1 for a time t_1 , the evolution period. During τ' , the mixing period, some of the evolved coherence is converted to magnetization by the action of the propagator $V(\tau')$. The resultant magnetization is observed during the detection period t_2 as it evolves under \mathcal{H}_2 . A multiple-quantum f.i.d. may be obtained by recording the intensity of the magnetization at a particular t_2 as a function of t_1 . Its Fourier transform is the multiple-quantum spectrum.

Suppressing constants and neglecting relaxation, the multiple-quantum f.i.d. at $t_2 = 0$ is:

$$\begin{aligned} S(\tau, t_1, \tau') &\equiv \text{tr} \{ \rho(\tau + t_1 + \tau') I_z \} \\ &= \text{tr} \{ V \exp(-i\mathcal{H}_1 t_1) U I_z U^+ \exp(i\mathcal{H}_1 t_1) V^+ I_z \} \\ &= \text{tr} \{ \exp(-i\mathcal{H}_1 t_1) U I_z U^+ \exp(i\mathcal{H}_1 t_1) V^+ I_z V \}. \end{aligned} \quad (4)$$

Define the quantities

$$\begin{aligned} I_z(-\tau') &\equiv V^+ I_z V = \sum_{ij} z_{ji}(-\tau') |j\rangle \langle i|, \\ \rho(\tau) &\equiv U I_z U^+ = \sum_{ij} \rho_{ij}(\tau) |i\rangle \langle j|, \end{aligned}$$

where the bras and kets are the eigenstates of \mathcal{H}_1 . The eigenvalues are in frequency units so that $\mathcal{H}_1|i\rangle = \omega_i|i\rangle$. The trace expanded on this basis is

$$S(\tau, t_1, \tau') = \sum_{ij} \rho_{ij}(\tau) z_{ji}(-\tau') \exp(-i\omega_{ij} t_1), \quad (5)$$

where $\omega_{ij} = \omega_i - \omega_j$.

The experimental time needed to achieve a desired signal: noise ratio will be proportional to signal energy or the squared magnitude of the Fourier coefficients in (5). For a resolved, non-degenerate transition at frequency ω_{ij} this is $|\rho_{ij}(\tau)|^2 |z_{ji}(-\tau')|^2$.

(c) *Enhancement of the selected transitions*

To see how selective excitation may be used to maximize this quantity for a typical desired transition, some statistical considerations are needed. The coefficients are constrained by the relations

$$\left. \begin{aligned} \sum_{ij} |\rho_{ij}(\tau)|^2 &= \text{tr}(\rho^2(\tau)) = \text{tr}(I_z^2), \\ \sum_{ij} |z_{ji}(-\tau')|^2 &= \text{tr}(I_z^2(-\tau')) = \text{tr}(I_z^2), \end{aligned} \right\} \quad (6)$$

which simply state the conservation of the norm of an operator under unitary transformation.

If the sums in (6) have N_t terms that are possibly non-zero, then the average term is

$$|\overline{\rho_{ij}(\tau)}|^2 = |\overline{z_{ji}(-\tau')}|^2 = \text{tr}(I_z^2)/N_t. \quad (7)$$

Assuming no correlation between the magnitudes of the factors, the average signal energy for a transition is

$$|\overline{\rho_{ij}(\tau)}|^2 |\overline{z_{ji}(-\tau')}|^2 = \{\text{tr}(I_z^2)/N_t\}^2. \quad (8)$$

In fact, U and V can always be designed to give a positive correlation between the factors on the left, but (8) suffices as a lower bound.

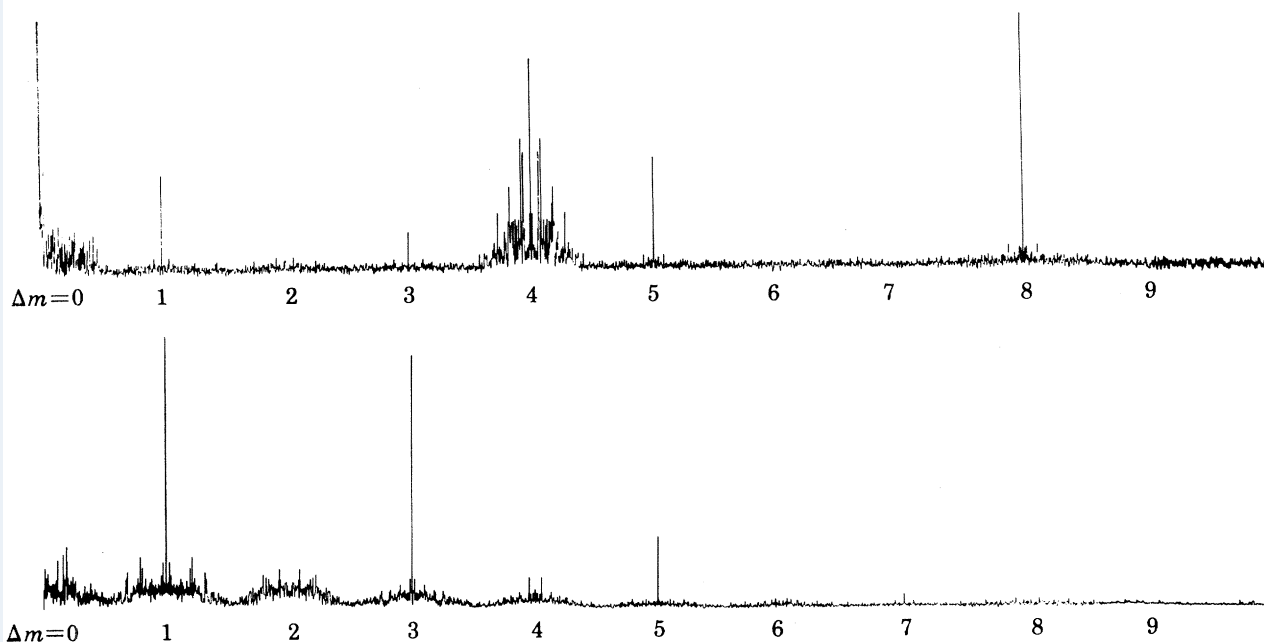


FIGURE 3. Comparison of the $4k$ -selective (a) and the non-selective (b) multiple-quantum spectra of n -butylbromide orientated in a nematic liquid crystal. Spectrum a is obtained from the $4k$ -selective experiment and shows an enhancement for the $\Delta m = 4$ region.

The role of selective excitation is now clear. It is used to reduce the number of transitions, thereby increasing the average energy available to each. To satisfy (7), both preparation and mixing propagators, U and V , should be selective for the same N_t elements of the density operator.

The improvement in signal energy possible with selective excitation will, by (8), be the square of the factor by which N_t can be reduced. The expected relative gain, G , in signal amplitude is the first power of this factor. For a system of N spins $\frac{1}{2}$ without any symmetry, the non-selective experiment will involve all elements of the density operator, giving $N_t = 4^N$. The nk -quantum selective experiment has $N_t = \sum_k \binom{2N}{N+nk}$, where the integer k runs over all values such that $|nk| \leq N$.

(d) *Illustrative experimental spectra of orientated n -butylbromide*

Figure 3 shows a non-selective and a $4k$ -selective spectrum of the nine-proton system of n -butylbromide orientated in a nematic liquid crystal. The ratio of signal amplitudes calculated as the ratio of N_t values is $G = 4.0$. The normal single-quantum spectrum of this system is essentially intractable. The selective spectrum shows an enhancement of the normally very weak four- and eight-quantum lines. The experimental enhancement for $\Delta m = 4$ in figure 3 is in fact

observed to be better than the estimated value of $G = 4.0$. This can be explained by recalling the linear approximation of (2). While zero-, four- and eight-quantum terms survive the sum over phase, the zero-quantum terms do not effect the density operator in the linear régime, because all such terms commute with the initial condition I_2 . Thus it is inconsistent to include all of the numerous zero-quantum elements in the calculation for N_t . A more reasonable estimate is to include only the diagonal elements, since these are initially non-zero. This amounts to replacing the $k = 0$ term $\binom{2N}{n}$ in N_t by 2^N . This leads to a predicted $G = 15$. For $\Delta m = 4$ the experimental G indeed lies between these two estimates. Clearly, the optimum approach is to use a more sophisticated excitation sequence that also eliminates the zero-quantum terms (Warren *et al.* 1980*b*).

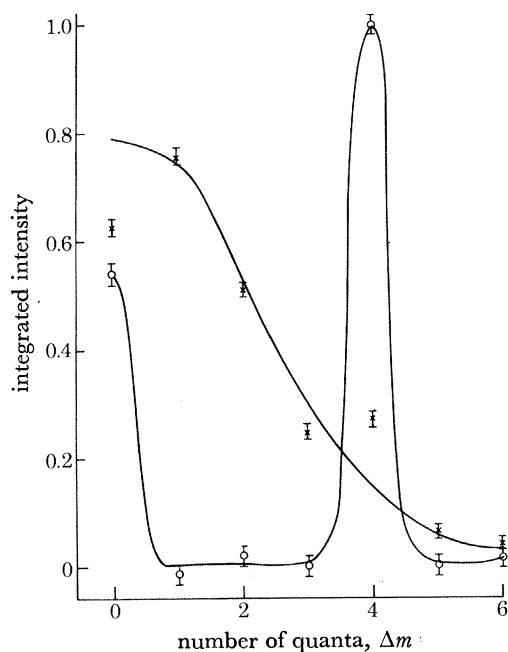


FIGURE 4. Integrated intensities of the multiple-quantum spectra of orientated benzene for each value of Δm . Each \times indicates the integrated intensity for a particular Δm obtained from the non-selective experiment. Each \circ indicates the integrated intensity for a particular Δm obtained from the $4k$ -selective experiment. Note the sharp peak at $\Delta m = 4$ for the $4k$ -selective experiment.

(e) *Selective and non-selective intensity distributions in orientated benzene*

The signal:noise ratio for the non-selective excitation of high multiple-quantum transitions in *n*-butylbromide is poor, and quantitative calculation of the gain from selective excitation is therefore difficult. This problem is less severe for orientated benzene where every symmetry-allowed transition can be observed non-selectively (Wemmer 1979; Drobny *et al.* 1979). Figure 4 shows the integrated intensity of the multiple-quantum spectra for each value of Δm , in non-selective and $4k$ -quantum selective experiments. In the non-selective experiment the intensities correspond roughly to a Gaussian distribution, because the number of allowed transitions decreases as Δm increases (Wemmer 1979). The intensity distribution for the selective experiments is sharply peaked at $\Delta m = 0$ and $\Delta m = 4$. Again, zero-quantum transitions appear only in non-linear terms and can be eliminated. In addition, many zero-quantum transitions are forbidden in selective experiments; for example, none of the zero-quantum transitions in the $m = 0$ manifold are allowed, because four-quantum operators cannot connect these states to any others, so

the nonlinear terms are never produced. All transitions corresponding to other values of Δm are strongly attenuated. The experimental results of figure 4 are a sum over all lines and therefore over all irreducible representations. The three pairs of $\Delta m = 4$ lines that do not fall at the centre of that order are of A_1 symmetry. The experimental gain for those lines due to selective excitation is $G = 5.6$. The statistical estimates from the available magnetization within the A_1 states are $G = 4.4$ (zero-quantum coherences included) and $G = 6.7$ (populations only included).

(f) *Comments on signal enhancement by selective excitation*

The examples discussed demonstrate the usefulness of selective excitation for increasing the signal of selected orders of transitions and the qualitative validity of the simplest statistical approach of assuming that the initial magnetization is distributed among selected transitions. A few caveats and extensions are needed. The magnetization available to the selected transitions is not always the full initial magnetization, but only that due to populations that are perturbed by the propagators U and V . The linear approximation of (2) is not necessary as sequences can be designed that are selective to arbitrary powers of time. These matters are discussed further by Warren *et al.* (1980*a, b*). Finally, the gain calculations presented here are for the case where the signal consists only of magnetization present at $t_2 = 0$. For a full two-dimensional experiment (Aue *et al.* 1976) a dependence on \mathcal{H}_2 is expected and this will be presented elsewhere.

4. INFORMATION CONTENT OF THE HIGH-QUANTUM SPECTRA

(a) *The N -quantum spectrum*

A general realm of application for multiple-quantum spectroscopy with selective excitation is the deduction of the evolution period Hamiltonian \mathcal{H}_1 from the relatively simple and well resolved high-quantum spectra. The highest-order spectrum is always a single line whose position is determined by the sum of the chemical shifts of the coupled spins, but is independent of the spin couplings. This approach to chemical shift measurements may complement multiple-pulse techniques. The dipolar Hamiltonian is avoided, rather than eliminated, and the shift tensor observed is a molecular, rather than a single particle, property.

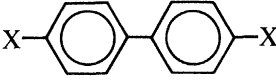
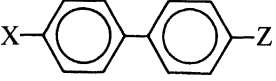
(b) *$(N-1)$ and $(N-2)$ quantum spectra*

Our interest here, however, is in the dipolar couplings themselves. When there are negligible chemical shift differences between the coupled spins, it is particularly simple to evaluate the amount of information about the couplings present in the $(N-1)$ and $(N-2)$ spectra of N spins $\frac{1}{2}$. The spectra consist of pairs of lines symmetrically displaced about a common centre. For the $(N-2)$ spectrum, there is a highly degenerate centre line as well. The number of pairs is listed in table 1 for several protonated species. The symmetry used is that which would be appropriate in the presence of motional averaging of the couplings, as in a liquid crystal solvent. The number of line pairs in the $(N-2)$ spectrum is always equal to the number of distinct *ordered* pairs of protons.

In contrast, the number of dipolar couplings is equal to the number of distinct pairs of protons and may also be viewed as the number of isotopically disubstituted molecules that would be needed to measure these couplings one at a time. Since the number of distinct ordered pairs is greater than or equal to the number of distinct pairs, the $(N-2)$ spectrum always contains enough information to allow a spectral fit by iteration on the dipolar couplings.

Finally, we mention that there is information in the relaxation of the high-quantum spectra that may not be readily available from normal one-quantum relaxation studies. Examples are correlated paramagnetic relaxation (Tang & Pines 1980*a*) and correlated methyl group rotation (Tang & Pines 1980*b*).

TABLE 1. DIPOLAR INFORMATION IN HIGH-QUANTUM SPECTRA

molecule or moiety	formula	number of protons, N	line pairs in $\Delta m = N-1$ spectrum	line pairs in $\Delta m = N-2$ spectrum	distinct dipolar couplings
benzene	C_6H_6	6	1	3	3
symmetric <i>para</i> -disubstituted biphenyl		8	2	10	7
unsymmetric <i>para</i> -disubstituted biphenyl		8	4	20	12
<i>n</i> -butyl chain	$R-(CH_2)_3-CH_3$	9	4	22	13
cyclopentane	C_5H_{10}	10	1	5	5

This work was supported by the Division of Materials Sciences, Office of Basic Energy Sciences, U.S. Department of Energy, under contract no. W-7405-Eng-48. We wish to thank Ms Terry Judson for her assistance in the preparation of the manuscript.

REFERENCES (Drobny *et al.*)

- Aue, W. D., Bartholdi, E. & Ernst, R. R. 1976 *J. chem. Phys.* **64**, 2229–2246.
 Bodenhausen, G., Vold, R. L. & Vold, R. R. 1980 *J. magn. Reson.* **37**, 93–106.
 Drobny, G., Pines, A., Sinton, S., Weitekamp, D. P. & Wemmer, D. 1979 *Faraday Symp. chem. Soc.* **13**, 49–55.
 Haebleren, U. 1976 *High resolution NMR in solids: selective averaging*. New York: Academic Press.
 Hatanaka, H. & Hashi, T. 1975*a* *J. phys. Soc. Japan* **39**, 1139–1140.
 Hatanaka, H., Terao, T. & Hashi, T. 1975*b* *J. phys. Soc. Japan* **39**, 835–836.
 Pines, A., Wemmer, D., Tang, J. & Sinton, S. 1978 *Bull. Am. phys. Soc.* **23**, 21.
 Tang, J. & Pines, A. 1980*a* *J. chem. Phys.* **72**, 3290–3297.
 Tang, J. & Pines, A. 1980*b* *J. chem. Phys.* **73**, 2512–2513.
 Vega, S. 1978 *J. chem. Phys.* **68**, 5518–5527.
 Vega, S., Shattuck, T. W. & Pines, A. 1976 *Phys. Rev. Lett.* **37**, 43–46.
 Warren, W. S., Sinton, S., Weitekamp, D. P. & Pines, A. 1979 *Phys. Rev. Lett.* **43**, 1791–1794.
 Warren, W. S., Weitekamp, D. P. & Pines, A. 1980*a* *J. magn. Reson.* **40**, 581–583.
 Warren, W. S., Weitekamp, D. P. & Pines, A. 1980*b* *J. chem. Phys.* **73**, 2084–2099.
 Wemmer, D. 1979 Ph.D. thesis, University of California, Berkeley.
 Wokaun, A. & Ernst, R. R. 1977*a* *J. chem. Phys.* **67**, 1752–1758.
 Wokaun, A. & Ernst, R. R. 1977*b* *Chem. Phys. Lett.* **52**, 407–411.